Current Biology, Vol. 13, R734–R744, September 16, 2003, ©2003 Elsevier Science Ltd. All rights reserved. DOI 10.1016/S0960-9822(03)00653-5

Biomimetic Systems for Studying Actin-Based Motility

Review

Arpita Upadhyaya and Alexander van Oudenaarden

Actin polymerization provides a major driving force for eukaryotic cell motility. Successive intercalation of monomeric actin subunits between the plasma membrane and the filamentous actin network results in protrusions of the membrane enabling the cell to move or to change shape. One of the challenges in understanding eukaryotic cell motility is to dissect the elementary biochemical and biophysical steps that link actin polymerization to mechanical force generation. Recently, significant progress was made using biomimetic, *in vitro* systems that are inspired by the actin-based motility of bacterial pathogens such as *Listeria monocytogenes*. Polystyrene microspheres and synthetic phospholipid vesicles coated with proteins that initiate actin polymerization display motile behavior similar to *Listeria*, mimicking the leading edge of lamellipodia and filopodia. A major advantage of these biomimetic systems is that both biochemical and physical parameters can be controlled precisely. These systems provide a test bed for validating theoretical models on force generation and polarity establishment resulting from actin polymerization. In this review, we discuss recent experimental progress using biomimetic systems propelled by actin polymerization and discuss these results in the light of recent theoretical models on actin-based motility.

Introduction

Cell locomotion is a highly complex process involving various biochemical and biophysical elements. Eukaryotic cells move by coordinating changes in shape and adhesivity to the substrate in response to environmental stimuli [1]. Motion is usually associated with motor proteins that convert chemical energy into mechanical work. However, there is increasing evidence that polymerization of proteins itself generates mechanical forces. Actin is an ubiquitous protein polymer in eukaryotic cells and its polymerization alone is thought to provide the force required to deform cell membranes in order to change their shape or to propel the cell body [2,3]. Within the cell, actin polymerization is tightly regulated by a host of actin associated proteins. As actin is involved in diverse cellular phenomena and signaling pathways, identifying the biochemical steps that lead to force generation has been difficult. To obtain a better understanding about the nature of the forces and the biophysical mechanism of force generation, it is important to use a system that facilitates quantitative investigation of the key processes.

Massachusetts Institute of Technology, Department of Physics, Cambridge, MA 02139, USA. E-mail: avano@mit.edu

The past 10 years have seen remarkable advances in our understanding of the molecular basis of actin-driven cell motility [4,5]. A major breakthrough was the discovery that intracellular bacterial pathogens, such as *Listeria,* use the actin machinery to propel themselves [6–8]. Notably, a single bacterial protein, ActA, is sufficient to induce motility of *Listeria* in a medium containing a few other actin associated proteins from the host cell's cytoplasm [9,10]. *Listeria* has, therefore, become a preferred model system that has been instrumental in determining the biochemistry and biophysics of the actin machinery. A further degree of simplification was achieved by the reconstitution of *Listeria* motility with purified proteins [10]. These experiments provide strong evidence that polymerization suffices to push a load in the absence of any motor proteins.

The *in vitro* motility system of *Listeria* was further simplified when polystyrene beads coated with ActA [11,12] or similar proteins [13–15] were shown to exhibit the same characteristic motion as *Listeria*. It appears that actin polymerization can be used to move any object coated with any of such proteins [16]. This finding paves the way for biophysical experiments to study the mechanism of force generation, as it allows for a systematic variation of parameters and direct comparison with models. More recently, experiments using phospholipid vesicles propelled by actin polymerization have provided a conceptual advance in our understanding of the force generation mechanism [17,18]. Figure 1 shows a schematic representation of the three different kinds of cargo used in biomimetic studies of actin driven motility.

One of the key challenges is to understand how actin polymerization on the single filament level can lead to force generation on the mesoscopic level. Theoretical models, which can be compared to experiments, are crucial in unraveling the exact biophysical mechanisms. Several models have been proposed over the years, each of them addressing phenomena on different scales. One class of models is microscopic in nature and describes polymerization on the level of single filaments or populations of filaments over a scale of tens of nanometers near the surface of the load ([19–22], Mogliner and Oster, this issue). On a larger scale models describe the entire actin as a continuous elastic gel [23] that deforms due to stress induced by growth and interactions with the load. Biomimetic experiments with artificial cargo will be instrumental in testing the predictions of these different models.

Here, we will review the recent advances in the study of actin based motility with artificial cargo or biomimetic systems: (i) actin polymerization alone can generate sufficient force to push a load; (ii) the polymerization motor is an extremely strong propulsive engine not limited by the hydrodynamic drag; (iii) the actin gel is connected to the surface; (iv) mechanical properties of flexible loads can play an important part

in regulating the dynamics. In the light of these studies we will attempt to integrate all the information about the physical basis of the force generation and raise questions for future research.

Reconstitution of Motility: Polymerization Can Push

In the 1980s, it was discovered that actin is responsible for the intracellular movement of some bacterial pathogens. *Listeria* invades the cell and hijacks the actin machinery of the host cell to propel itself through the cytoplasm. Actin polymerizes on the surface of the bacterium, forming a dense cloud around it. Subsequently, the actin cloud becomes polarized into a comet tail made of an oriented, cross-linked network of actin filaments, with their fast growing, barbed ends pointing towards the bacterium. As the comet tail elongates, it pushes the bacterium forward at a fairly large speed, approaching 1 μm/s.

Basic Biochemistry of* Listeria *Motility

Listeria is a good model system to study actin based motility, as the comet tail represents a simplified lamellipodium and the bacterial surface imitates the plasma membrane at the leading edge. The only bacterial protein required for motility is ActA, which is distributed asymmetrically on the bacterial surface [9]. ActA is functionally similar to the WASP family of proteins, which are associated with the lamellipodia of moving eukaryotic cells. Beads coated with ActA [11,12], WASP [13], N-WASP [15], or the VCA domain of WASP [14] show similar motility. Remarkably, only a set of five purified proteins is required for reconstitution of sustained *Listeria* and bead motility. ActA and N-WASP are activators of the Arp2/3 complex, which initiates polymerization at the barbed end of filaments by branching. The regulatory domains of WASP proteins associate with several signaling molecules, such as small GTPases [24–26]. The binding of such signaling molecules regulates the localization of WASP proteins to sites on the plasma membrane, at which the Arp2/3 mediated actin response is initiated. The only additional proteins required for formation of the comet tail are capping protein and ADF/cofilin. Elongation of filaments occurs at the barbed ends and pushes the load forward. Capping protein caps free barbed ends and inhibits further elongation. Actin depolymerizing factor (ADF) or cofilin causes disassembly of actin polymers from the older parts of the comet tail, thus supplying a steady pool of monomers for elongation of the leading edge (see Figure 2, Mogilner and Oster, this issue). Further details of the molecular mechanism of actin polymerization can be found in several recent reviews [4,5,8,16].

Polymerization Can Push

Even though the biochemistry of the actin machinery is well understood, the biophysics of the force generation are yet to be resolved. One of the most important conclusions from experiments on non-biological loads moving in cell-free assays is that actin polymerization is sufficient to generate a force that can move micron-sized loads. *In vitro*, actin filaments are long and flexible [27–29] and incapable of generating a significant pushing force without buckling. To generate a force that can push forward, the polymerizing filaments must be bound to the substratum or be cross-linked in some way, otherwise polymerization would result merely in a rearward movement of the filaments.

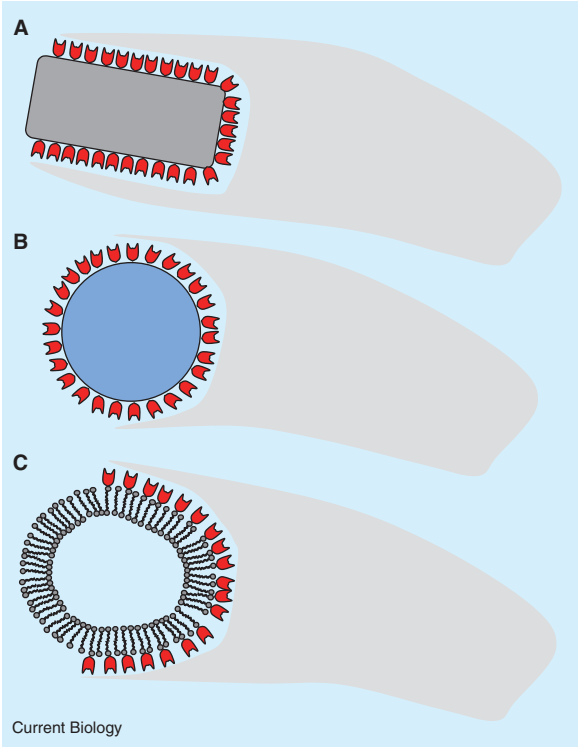

Figure 1. Biological and biomimetic cargo transported by actin polymerization.

The gray comet tails depict the actin gel and the red symbols denote the protein ActA. For *Listeria* (A), ActA is asymmetrically distributed on the cell membrane, whereas on microspheres (B) ActA is uniformly distributed. Phospholipid vesicles (C) coated with ActA are deformed from their spherical equilibrium shape by the squeezing of the actin gel (Box 1).

In cells, most of the actin near the lamellipodium forms a dense cross-linked meshwork [30]. The comet tail of *Listeria* or beads also consists of an oriented, cross-linked network of actin filaments with their barbed ends pointing towards the load [31]. The Arp2/3 complex initiates filament branching and serves as a cross-linker, as is shown by experiments using a fluorescently labeled version of the Arp2/3 complex [15]. A preferred 70 degree angle between branches results in filaments being tilted with respect to the membrane rather than being perpendicular [32–34]. The typical spacing between branches is tens to a few hundred nanometers. Capping of the growing barbed ends limits filament length and ensures that filaments are short and stiff rather than long and flexible and, therefore, more effective at exerting a force. From the bending stiffness of actin filaments, it was theoretically shown that the length of the 'pushing' filament must be in the range of 30–150 nm [19]. For efficient force generation and optimum motility, there must be a balance between the relative rates of elongation, branching, capping and disassembly.

Force-Velocity Relations

The main biophysical objective is to understand the nature and magnitude of the forces that actin based polymerizing structures can generate. Theoretical studies predict the force-velocity relation for an elongating polymer [35] and the force produced by a polymerizing microtubule has also been measured [36]. However, the force generated by a growing actin filament is yet to be measured. Because the polymerization of an ensemble of actin filaments can convert chemical energy to mechanical work, it can be considered a 'motor'. To probe the energetics of the polymerization motor, recent experiments have obtained the first measurements of a force-velocity relation.

McGrath *et al.* [37] studied *Listeria* motion in a highly viscous environment. Increasing the viscoelastic modulus by 500-fold only slowed down the bacteria by a factor of about 20. They measured the force-velocity curve of *Listeria* motility, and found it to be highly curved, almost biphasic, i.e. displaying two distinct behaviors at small and large loads. With small loads (10–20 pN), there was a significant decrease in velocity (from ~70 nm/s to ~10 nm/s), whereas large loads (up to ~200 pN) decreased the velocity slowly with force. This force-velocity curve limits the theoretical models that can be used to explain the data, as will be discussed in a later section. Furthermore, the density of the actin tail increased with increasing viscosity or external load. A small increase in actin density (1.6-fold) corresponded to a much larger force generation (20-fold increase). These results suggest that force generation depends sensitively on the structure of the actin tail. This increase in actin density also suggests possible 'self-strengthening' of *Listeria* in environments of high resistance. *Listeria* trajectories consist of molecular-sized steps, the duration of the steps correlates with speed, while the step-size is not correlated with speed. In other words, with increasing external load the stepping frequency decreases, but the distance per step remains unaffected.

Another study by Wiesner *et al.* [15] investigated the motility of N-WASP coated beads in a reconstituted motility assay and observed no slowing down of the beads even when the viscosity was increased 4000-fold. The beads slowed down by less than a factor of 2, if the viscosity was increased by a factor of 10^5. The resulting force-velocity curve is very shallow compared to the steeper, highly curved force-velocity relation of McGrath *et al*. As the velocity is barely decreased by external load, it appears that extremely large forces are developed by actin polymerization. The authors interpret their results in terms of a strong internal force that opposes the motion. Forces of up to 50 pN fail to slow down the bead, indicating that the forces (propulsive as well as retarding) must be larger than 50 pN and possibly in the nanonewton range.

The apparent differences between the observations by McGrath *et al.* [37] and Wiesner *et al.* [15] must be resolved to obtain a consistent picture of actin driven motility. Indeed, many of the details of the two experiments are quite different, as for instance the former was done in a complete cell extract, whereas the latter used a chemically well defined medium with purified proteins.

Characterization of Bead Velocities

Apart from external drag, several other factors in the experimental system may affect the velocity of beads. In particular, modulating parameters that affect the structure of the actin tail will be important. Cameron *et al.* [11] found that ActA coated beads in cell extract move at about 0.1 μm/s, comparable to *Listeria* movement in similar extracts. *In vivo, Listeria* move with velocities of about 0.3 μm/s . For beads in the range of 0.2 μm to 1 μm, they observed that smaller beads were moving more slowly with the velocity being independent of the surface density of ActA. The fluorescence intensity of the actin tail, corresponding to its actin content, increased with increasing ActA density. Bernheim-Groswasser *et al.* [14] used beads coated with VCA (the active subdomain of WASP) at saturating density and showed that the mean bead velocity (the fastest being 0.01 μm/s) is inversely proportional to the bead diameter, in contrast to Cameron *et al.*'s observations. Bernheim-Groswasser *et al.* used a defined medium with purified proteins. Studying beads of sizes that ranged from 1–7 μm, they observed qualitatively different kinds of motion ranging from smooth to saltatory. Wiesner *et al.* [15] characterized the motion of N-WASP coated beads, also in purified protein buffer. A steady-state velocity (between 0.01 and 0.05 μm/s) was reached after about 10 min of incubation. The bead velocity increased with N-WASP density until it reached a plateau in the range of 2.8–5.6 nm spacing between N-WASP molecules. This could signify that a minimum spacing is required between N-WASP molecules for the most efficient propulsion. The amount of actin in the tail also increased with N-WASP density on the bead surface. Wiesner *et al.* inferred from their results the existence of a force that opposes bead propulsion. As they find that bead velocity does not decrease upon large increases in external viscosity, they postulate that the opposing force is an internal force, which also increases with increasing filament number. Increasing the concentration of the capping protein (gelsolin) caused a steep decrease in bead velocity at any given N-WASP and Arp2/3 complex density. Actin structures were found to be poorly branched at low gelsolin and highly branched at high gelsolin concentrations. It is interesting to note that the bead velocities are much smaller in the purified medium as compared to the extracts. The extracts potentially contain additional factors that might increase the propulsion speed.

Forces Generated by Actin

Stress in the Actin Gel

Over the last four years, experiments on *Listeria* and beads have allowed for a systematic variation of parameters and have led to a better understanding of the biophysical mechanism of actin based motility. It is clear that the structure of the actin tail will be an important determinant of the motion. Gerbal *et al.* [38] found that the actin filament tail behaves like an elastic gel, which is consistent with the densely cross-linked structure observed in electron microscopy images [31]. The mechanical properties of the actin gel are important in determining the nature of the forces that will be generated. The elastic properties of

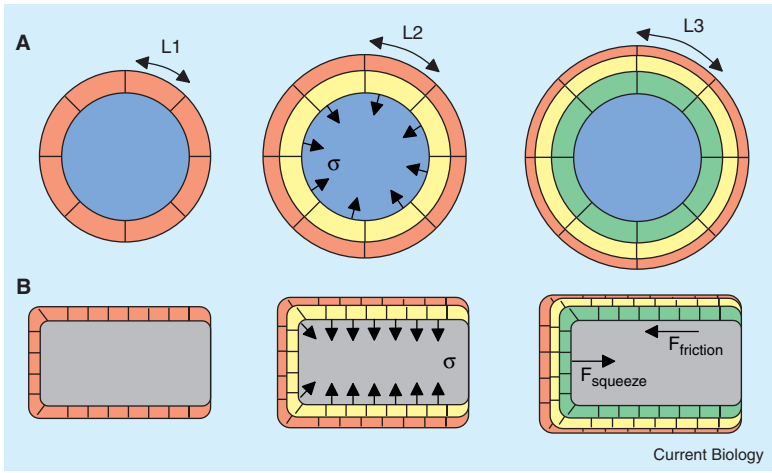

Figure 2. The build-up of elastic stress during growth of the actin gel around a curved surface.

(A) A bead coated with ActA initiates the growth of an actin gel layer (red). As the polymerization progresses, a second layer (yellow) is created between the bead surface and the preexisting actin gel layer, resulting in stretching of the initial gel ($L_2 > L_1$). The stretching results in a build-up of stress σ at the bead surface. As the thickness of actin gel around the bead increases ($L_3 > L_2$), the stress increases, ultimately leading to a vanishing actin polymerization rate at the bead surface (red circle) [39]. (B) In the case of *Listeria* the build-up of the elastic stress results in a resultant propulsive squeezing force ($F_{squeeze}$) that is balanced by a friction force ($F_{friction}$) due to the attachment of the actin gel to the bacterium body.

the comet tail have been studied by measuring its response to stress applied with optical tweezers [38]. The elastic modulus of the tail was estimated to be in the range 10^3–10^4 Pa, but further experiments are required to characterize how the elastic properties of the gel are altered by changing parameters such as actin density or cross-linking density. The forces that are generated are constrained by the elasticity of the gel and the mechanical properties of the load. Some theoretical models have focused on the elastic nature of the actin gel and postulated a build-up of significant stress in the gel during growth of actin filaments around beads or *Listeria* [23,39] (Figure 2). The first evidence of stress in the gel was provided by Noireaux *et al.* [39], who showed that actin shells grow on ActA coated beads only up to a limited thickness and that the thickness of the shells increases with the bead radius. Calculations demonstrated that the gel must sustain elastic stress as a consequence of the spherical geometry and that this limits the growth of the filaments. An elastic model [23] of the comet tail describes how the addition of filaments to the tail produces strains that distort the actin gel. The relaxation of these strains propels the bacterium (Figure 2) and the scale of the predicted elastic forces is in the range of nanonewtons. Thus, these analyses highlight the importance of the collective behavior of a network of actin filaments working together to generate a force.

Vesicles as Model Systems

As the response of the actin gel to stress is difficult to measure, experimental validation of these concepts was lacking and the spatiotemporal distribution of forces had not been observed directly. Because bacteria and beads do not change their shape in response to an external force, it became important to develop a biomimetic system that would deform under an applied force. Phospholipid bilayer vesicles are an obvious choice, as they resemble the plasma membrane at the leading edge of cells.

Physically, lipid membranes are fluid under shear, but can resist bending and stretching forces. This gives rise to measurable elastic moduli which have been well characterized [40,41]. Vesicle membranes deform significantly upon external forces and several experiments have demonstrated that actin polymerization can deform a membrane [42–44]. Miyata and Hotani [42] encapsulated actin inside vesicles and recorded the membrane protrusions resulting from polymerization of actin. These observations show that elongation of proteins by polymerization is sufficient to deform a membrane. As the shape changes can be used to deduce the forces acting on a vesicle, vesicles can be used as sensitive spatial and temporal force transducers. Actin polymerization has been observed to power the motility of lipid membrane structures such as endocytic vesicles [45], endosomes and lysosomes in the cytoplasm of fertilized *Xenopus* extracts, and synthetic vesicles containing phosphatidylinositol-4,5-biphosphate [46,47]. Membrane vesicles propelled by major sperm protein have also been observed in cell-free extracts [48]. However, these lipid vesicle systems were not used to obtain a quantitative measure of the forces.

Vesicles as Force Sensors

Experiments by Upadhyaya *et al.* [17] and Giardini *et al*. [18] showed that vesicles coated with ActA move by generating *Listeria*-like comet tails and are deformed into tear-drop shapes. The force stretches the vesicle surface, establishing a membrane tension, and causes a decrease in vesicle volume by squeezing water out, which generates an osmotic pressure. The competition between the stretching stress (inward) and the osmotic pressure (outward) as well as the stress due to polymerization determine the shape of the vesicle. The authors found that a measure of the polymerization stress can be obtained by analyzing the curvature of the vesicle contour, a purely geometric quantity (see Box 1). The characteristic teardrop shape implies that the sides of the vesicle experience strong compression or squeezing forces, whereas the trailing edge of the vesicle is pulled backwards by retractile forces at the center of the comet tail. It is important to note that the forces shown in Figure 3 are exerted by the actin gel to maintain the deformed shape of the vesicle. These

Box 1

Phospholipid Vesicles as Force Transducers.

The equilibrium shape of a vesicle under external load is determined by minimizing the energy required to bend and stretch the membrane and to change the volume of the vesicle against an osmotic pressure. As the bending energy is much smaller than the energies required to stretch the membrane and to decrease the vesicle volume, the bending of the membrane can be neglected [37]. In the absence of the actin gel, most vesicles assume a spherical shape. In response to polymerization of the actin gel the vesicles are significantly deformed into more elongated, tear-drop shapes as sketched in Figure 3.

As the vesicle deforms, an outward osmotic pressure Π develops due to a decrease in volume. The volume decrease is accompanied by an increase in area, as the membrane surface stretches, creating a membrane tension τ that induces stress pulling the membrane inward and restoring its original area. This tension is constant in the membrane, because the phospholipid bilayer is fluid. The stress due to stretching is given by:

$$\sigma=\tau(\kappa_1+\kappa_2)$$

where κ_1 and κ_2 are the principal curvatures of the membrane. At the spherical cap (Figure 3) this stretching stress is balanced by the osmotic pressure:

$$\Pi=-\sigma_{cap}=\tau\ \kappa_{cap}$$

However at any other point of the membrane, the sum of the osmotic pressure Π and the stress induced by stretching σ is balanced by the pressure exerted by the actin polymerization Σ. This leads to the simple result that the stress due to actin polymerization is the product of the tension τ and the curvature difference $\Delta\kappa$ between the actin-free region and any other point on the vesicle surface:

$$\Sigma=\Pi+\sigma=-\tau\ \Delta\kappa$$

Because the curvature at the side of the vesicle is less than the curvature of the spherical cap, the actin pressure is directed inward and squeezes on the vesicle. However, at the trailing edge of the vesicle the curvature is larger than at the spherical cap and, thus, the actin gel pulls on the vesicle (Figure 3).

forces are in the frame of reference of the vesicle and do not represent the forces required to move the vesicle forward. The actin gel grows in the forward direction and the net growth of the tail due to polymerization of filaments pushes the vesicle forward.

The forces generated by the comet tail at the membrane surface are relatively large. According to Giardini *et al.,* the total force generated by the comet tail is 0.4–4 nN. Most of the forces are exerted perpendicular to the direction of motion and contribute to the deformation of the vesicle; less than 10% of the force is translated into forward motion. Upadhyaya *et al.* found that the maximum compressive or protrusive forces on the sides of the vesicle are in the range of 3–4 nN/μm^2 while the maximum retractile forces are 6–8 nN/μm^2. The estimated magnitudes of these forces are consistent with other observations. Elastic analysis of the comet tail [23,38] predicts forces in the nanonewton range. Forces on the order of tens of piconewtons are not able to slow down *Listeria* motion. It has been impossible to stall moving *Listeria* or beads, either by using an optical trap or by increasing the viscosity of the medium by several orders of magnitude. Also lamellipodial stall forces are simliar and in the range of 2 nN/μm^2 [49]. The forces generated by actin polymerization are much larger than the force required to overcome hydrodynamic drag. A spherical vesicle with a radius of 1 μm moving through water at a speed of 1 μm/min experiences a drag force of only 3×10^{-7} nN. This drag force is 50×10^6 times smaller than the typical propulsive force due to actin polymerization. Even in the presence of a highly viscous cytoplasm and cytoskeleton the drag force is more than four orders of magnitude smaller than the polymerization force. Furthermore, bacterial pathogens move with a similar velocity inside the cytoplasm as they do *in vitro* in the much less viscous motility medium. Thus, the actin polymerization engine is an extremely strong motor with significant power in reserve. The full strength might be utilized, for example, by invading pathogens that have to penetrate the host cell's plasma membrane.

Actin is Connected to the Surface

Stepping of Vesicles

The spatial segregation of compressive and retractile forces on the vesicle surface suggests that there must be two populations of filaments: those that push the membrane and others that pull the membrane. The presence of a retractile force that pulls on the surface of the vesicle is not intuitive. How can we understand the existence of a 'pulling' force? The filaments that pull must be bound to the surface. There can be an effective force arising from the tensile stress that tethered actin filaments exert on the membrane surface. As a vesicle moves, its shape changes over time and, consequently, the spatial distribution of forces is not constant. The vesicle slowly elongates due to an increase in retractile stress exerted by the actin gel. A computational model [17] indicates that the squeezing as well as retractile forces increase as the vesicle elongates. These observations led to the conclusion that the deformed vesicle shape is maintained, because the vesicle is bound to the actin gel. The elongation is followed by a rapid relaxation into a spherical shape as the vesicle appears to be released from the comet tail. Repeated elongation and release lead to a remarkable stepping motility of vesicles. This discontinuous motility could be explained by strong binding to the tail and rapid release due to a catastrophic breaking of bonds. The forces estimated from vesicle shapes can be used to obtain an approximate strength of the binding between the comet tail and the membrane. Maximum retractile forces on the order of 5–10 nN/μm^2 imply rupture forces of 10–20 pN per filament [17].

Experiments using fluorescently labeled ActA [17,18] reveal an affinity between surface bound ActA and the actin comet. Even though it is apparent that the actin tail must be attached to the surface of the load, the details of this attachment are unknown. Neither the protein that must mediate the binding between ActA coated surfaces and actin, as F-actin has not been shown to bind ActA, nor the timescale over which such binding occurs are known. An actively polymerizing filament must be in contact with the surface as the ActA-Arp2/3 conjugate along with G-actin is required to initiate branching. These attachments might be transient, such that the growing filament is free to elongate. Simultaneously,

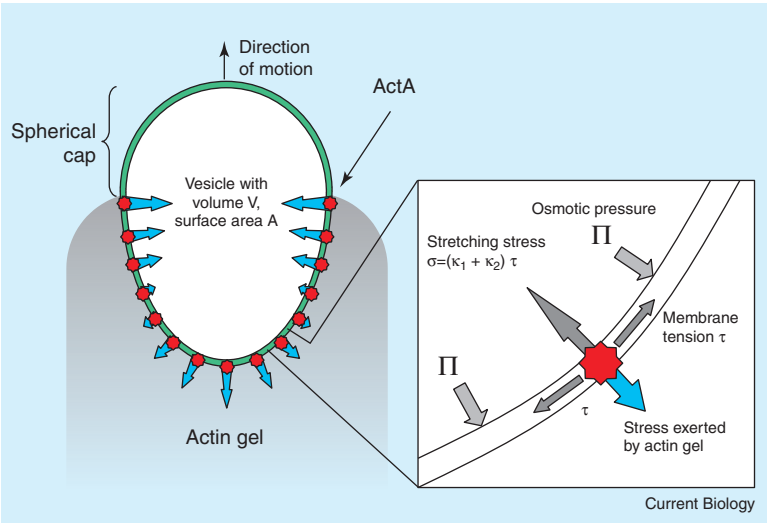

Figure 3. The stress exerted by the actin gel (blue arrows) on the membrane to balance the osmotic pressure and stretching stress is determined by the geometrical properties of the vesicle. As the vesicle deforms, its surface stretches, inducing a membrane tension that sets up stretching stresses that pull the membrane inward to restore its original surface area. Simultaneously, an osmotic pressure develops due to a decrease in volume. The stretching stresses depend on the local curvature of the membrane, whereas the osmotic pressure is global and independent of the membrane curvature. The local stress is the sum of the osmotic pressure and the stress induced by stretching.

there may be a fraction of strongly tethered filaments that are under increasing tensile forces as the surface is pushed forward by the 'free' elongating filaments. The unbinding might then be caused by 'fracture' after a critical tensile stress is exceeded. Alternatively, continuous binding and unbinding might be occurring at a shorter time scale, such that there is always a population of tethered filaments and one of non-tethered filaments. In this scenario, individual filaments would switch between the two states.

Stepping of Listeria

These ideas are supported by experiments on *Listeria* and beads, which indicate that actin must bind to the surface of the load. Analysis of *Listeria* motility with high spatial and temporal resolution using laser tracking [50] has revealed a step-like motion with steps of about 5 nm on average. This corresponds to the spatial periodicity of actin filaments and the size of an actin monomer. Moreover, within the cytoplasm, motile bacteria fluctuate about 20 times less than organelles or structures of similar size. This implies that the bacteria do not 'sense' the local cytoplasmic viscoelasticity and, therefore, must be attached to their actin tails. The authors propose that bacterial motion may be limited by binding to a few filaments that are under tension. Then 'slipping' would occur along these yielding a 5 nm periodicity [50]. Given that hundreds of filaments are involved, it is remarkable that such small steps are observed.

At a larger length and time scale, some mutants of *Listeria* are observed to undergo a 'hopping' motion with micron sized jumps and intervals of minutes between the jumps [51]. A similar stepping motion has been observed for VCA-coated beads [14]. Changes in the surface density of VCA or in the bead size caused a transition from smooth to 'hopping' motility. Increasing the bead size or decreasing the VCA concentration induced stepping motion. Direct experiments using optical tweezers have unsuccessfully tried to separate beads from the trailing comet tail, thus demonstrating the strong attachment between the bead and the tail [38]. Recent electron microscopy images have also provided clear evidence that filaments of the comet tail are indeed attached to the beads, as they show only a few filaments in contact with a bead at any given time and high variability between beads [52].

Symmetry Breaking and Polarization

One of the fundamental puzzles in cell motility is the origin of cell polarization to achieve directional motion, especially in the absence of any external signals. Directed motility requires actin filaments to be distributed asymmetrically and to polymerize in a spatially controlled manner in association with the cell membrane [53]. Experiments with reduced systems may provide us with important insight into how polarity develops, as the effects of external signals and the role of intrinsic mechanisms can be decoupled.

Symmetry Breaking in Beads

All examples of movement of artificial cargo show a preferred directionality of motion, as is evident in the formation of a single comet tail. In some cases there is an intrinsic asymmetry in the system: wild type *Listeria,* for instance, are covered only on one side with ActA. Hence, actin polymerizes on the part of the surface where ActA is present and spontaneously generates a comet tail in that direction (Figure 1). A few minutes after the addition of motility ingredients, motion is initiated. However, intrinsic asymmetry is not required for directional motion. Beads that are homogenously coated with ActA over their entire surface also move with a single comet tail [11–15]. The bead is encased in a meshwork of polymerizing actin filaments, which is observed as a 'cloud' around it. The bead fluctuates within this cloud and then suddenly shoots out in one direction.

There are some important differences between beads in extract [11] and beads in media containing purified proteins [14]. In extracts, the bead is entrapped in the actin cloud for about an hour after incubation before symmetry is broken, while in reconstituted media it takes only about 5–25 minutes, depending on bead size. In extracts, beads larger than 0.5 μm in diameter do not spontaneously generate a

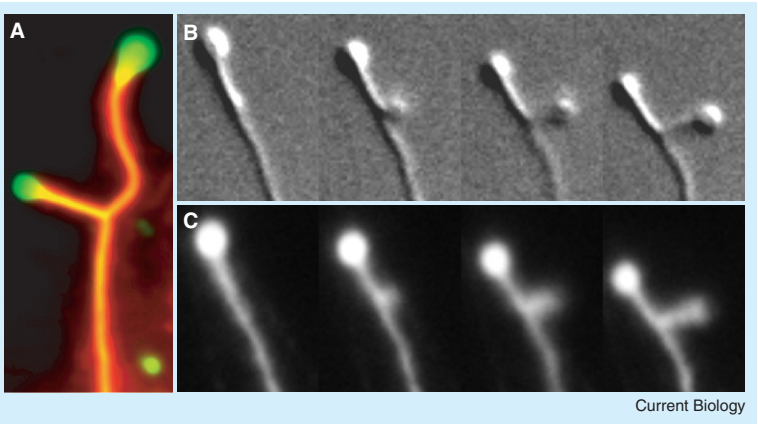

Figure 4. Spontaneous branching of a lipid tether.

(A) Fluorescence image of a branched tether. A fraction of the lipids was labeled with Oregon Green. The actin was labeled with rhodamine (red). Differential interference contrast microscopy (B) and fluorescently labeled actin (C) images illustrating a branching event. Images were taken at 30 s intervals.

comet tail and only a small fraction of the beads were motile [11,14]. In purified protein buffer, beads larger than 5 μm were able to move and all of the beads generated comet tails [14]. However, in extracts, asymmetric coating with ActA made larger beads (1–2 μm) motile and increased the probability of small beads forming comet tails [11] and smaller concentrations of ActA were required for movement when the coating was asymmetric.

Polarization of Lipid Vesicles

Interestingly, ActA coated lipid vesicles moving in cell extracts develop polarity very efficiently. Using fluorescently labeled ActA, images of moving vesicles show that the spatial distribution of ActA is highly polarized and is closely correlated with the position of the actin cup on the vesicle surface [17,18]. The ActA localizes on the posterior half of the vesicle and, as the actin changes its orientation around the vesicle, ActA redistributes to remain always associated with the actin. Because the lipid bilayer is fluid, diffusion of ActA conjugated lipids would be expected to create an initial uniform distribution of ActA on the surface. Subsequently, lateral movement of ActA bound lipids on the bilayer surface might facilitate the establishment of asymmetry. As the initial stages of this polarization have not been visualized, it is not clear whether part of the asymmetry is due to intrinsic self-aggregation properties of ActA and when the asymmetry is established. What is the active role of the actin filament dynamics as it interacts with the fluid membrane? The experimentally observed polarization indicates an affinity between ActA and actin filaments. This could be mediated by a third protein, such as Arp2/3 complex or VASP. Although there is no evidence of direct binding between F-actin and ActA, ActA has been shown to bind to actin filaments via the Arp2/3 complex and VASP [54–56]. Giardini *et al.* [18] found that the membrane deformation is not directly responsible for asymmetric ActA localization as also lipid monolayer coated beads showed ActA accumulation at the rear half of the beads. The polarization of ActA seems to be an actin-dependent process and may contribute to the establishment of a persistent directional motion. Further experiments are required to understand the mechanism of the generation of polarity and will be useful in deciphering the onset and maintenance of polarity in real cells.

Branching of Lipid Tethers

An unusual phenomenon observed in the vesicle motility system points to a novel example of symmetry breaking (A.U. and A.v.O., unpublished). Some vesicles draw out tubular lipid extensions, or tethers, as they are pushed forward by the actin tail. The tethers are drawn out behind the vesicle and they elongate in the same direction as the vesicle movement. The clump of lipids acts as a reservoir for the elongating tethers and membrane tubules of some tethered vesicles developed new tethers from the sides of pre-existing ones (Figure 4A). The branched membrane tubules are completely enclosed by a sheath of actin gel. Initially, the tether is uniformly covered by actin along its length. The formation of a branch is marked by the budding of a vesicle from one side of the tether (Figures 4B,C). In turn, the budded vesicle is propelled by actin and elongates as a tether. What triggers the nucleation of a branch from a smooth actin tail is unclear. It is probably due to small inhomogeneities on the actin sheath leading to a local weakening of the gel; this could enable the lipids to flow out of the sheath and the resulting asymmetry would propel the newly released lipids. Tether formation and branching are interesting analogs to the reticulation of the endoplasmic reticulum and to the tubulation of the Golgi apparatus during vesicle transport. Understanding the mechanism of their formation will be useful in completely recognizing the role of actin and actin dependent structures within the cell.

Modeling Actin Driven Motility

A major advantage of using biomimetic cargo to study the actin machinery is that it allows for quantitative experiments and systematic variation of parameters. This has facilitated comparison with predictive models and the testing of different hypotheses. The earliest models trying to explain how polymerization can push a load elaborated a Brownian Ratchet mechanism, building on thermodynamic ideas by Hill and Kirschner ([35], see Mogilner and Oster, this issue). The first implementation of this model by Peskin *et al*. [57] considered polymerization of filaments near a fluctuating load. The fluctuations of the load provide enough

space for monomers to intercalate at the tip of the growing polymer. As the filament elongates, it prevents (ratchets) the backward motion of the load and thus moves it forward. Modifications of this basic model include the effect of fluctuating elastic filaments [19].

The Tethered Filament Model

Subsequent experimental evidence on the structure and properties of the actin tail has allowed for a refinement of these models. Currently, two alternative scenarios are used to describe the growth and branching of actin filaments at the leading edge of a pre-existing array: the dendritic nucleation scheme, in which the rate of filament nucleation does not depend on the number of existing filaments and the autocatalytic branching model, in which the filament generation rate explicitly depends on the current filament density. The 'tethered' Brownian ratchet model [20] considers a dendritic nucleation scheme and accounts for the experimental fact that the load must be attached to the filaments. There are two populations of filaments: attached filaments are under tension and grow by *de novo* nucleation, whereas detached filaments are formed when the attached filaments dissociate. The detached filaments are the 'working' filaments which can generate a protrusive force and are lost by capping. The predictions of this model compare well with several experimental observations. The predicted propulsion velocity of 70 nm/s, for the nominal parameters, is in the same range as that obtained experimentally by Cameron *et al*. for ActA coated beads moving in cell extract. Furthermore, the bead velocity is almost independent of the density of ActA on the surface or the viscoelasticity of the cytoplasmic extract [11].

The model predicts that the velocity depends on the ratio of working to attached filaments rather than the total number of nucleation sites. A change in either the ActA or Arp2/3 concentration would affect the overall number of sites rather than the ratio and does, therefore, not affect the velocity. The model also predicts that smaller beads will move more slowly, concurrent with Cameron *et al.*'s observation. On the contrary, Bernheim-Groswasser's experiments [14] show that bead velocity is inversely proportional to bead radius. This apparent contradiction needs to be resolved. The force-velocity curve predicted by this model is steeply biphasic, as the velocity drops very fast for low forces below 20 pN and decreases more slowly with higher loads. Qualitatively this may be explained by the consideration that at high velocities filaments can detach rapidly and offer little internal resistance. At higher loads, and hence slower velocities, the attachments are more persistent and increase the internal resistance, thus further slowing down the bacterium. This is consistent with the force-velocity relation obtained by McGrath *et al*. for *Listeria* moving in extract [37]. In the model, the bead velocity is proportional to actin density and, therefore, the curve becomes shallower as the nucleation rate is increased. This and the sensitivity of the force velocity curve to changes in parameter values can be tested experimentally. However, Wiesner's flat force-velocity curve [15] cannot be explained by this model.

The Autocatalytic Branching Model

A different model by Carlsson [21,22] simulates actin filaments growing against an obstacle and compares the autocatalytic branching and dendritic nucleation schemes. The angular orientations of filaments are explicitly taken into account, whereas the tethering of filaments to the surface is not considered. The force-velocity curve obtained from the autocatalytic scheme predicts no decrease of velocity with increasing external load and is consistent with Wiesner's experiments on beads [15]. The physical explanation for this is that an increase in the external force causes the bead to slow down transiently. More new filaments can then be created to increase the filament density and result in the recovery of the initial velocity. This result depends entirely on the linear nature of the equations used and may have limited validity for several experimental situations.

Mogilner and Oster [20] have extended their model to include the 'autocatalysis' behavior. Working filaments become 'attached' with a certain association rate that might be determined, for example, by the concentration of the Arp2/3 complex. All attached filaments branch instantaneously such that when they dissociate, two working filaments are created for each filament that was initially attached. Their modified model does not explicitly include a branching rate and gives the same biphasic relation as before. This appears to be in contradiction to Carlsson's autocatalytic model, which predicts a flat relation. Closer observation reveals important differences between the two models. In Mogilner and Oster's model, the total rate of filament formation does not explicitly depend on the density of existing filaments. Furthermore, the association rate does not depend on the number of working filaments. In the limiting case of a very low number of working filaments, this might be a problem. They also do not consider the angular orientation of the filaments in the network. On the other hand, the model by Carlsson does not consider attachment between filaments and the surface, and thus, the external load is balanced by the total force exerted by the filaments, all of which can push. In contrast, in Mogilner and Oster's model there is an additional tension due to attached filaments. This leads to very different results for the force-velocity curves. Carlsson's model, extended to include the 'nucleation' scheme, produces a biphasic force-velocity relation similar to that in the tethered ratchet model. However, the physical origin of this type of relation is different for the two models. Importantly, under conditions of high filament density or attachment strength the force-velocity curve for the tethered ratchet model would be flat, as the velocities would be insensitive to the applied force. The experiments of Wiesner *et al.* might be operating in this regime. This underscores the importance of quantitative measurements of parameters such as filament densities and binding strengths.

It appears that the balance between branching rate and capping rate is important in determining the velocity. Experimentally, these can be controlled by varying the N-WASP and Arp2/3 concentration, to determine branching, and the concentration of capping

proteins, such as gelsolin. Experiments demonstrate that the velocity decreases sharply with increasing gelsolin concentration. Based on Carlsson's simulations [21], this implies that uncapping is not important and favors 'end-branching' of filaments. Furthermore, branching structures at low and high gelsolin are consistent with the autocatalytic branching model. Different branching versus capping rates can also lead to the different morphologies of actin arrays in lamellipodia and filopodia. Wiesner *et al*. [15] also found that the asymptotic velocity of beads does depend on the N-WASP surface density (unlike Cameron *et al*.'s results with ActA coated beads [11]) in that the bead velocity increases with N-WASP density up to a certain maximum.

Elastic Continuum Models

On a completely different scale models operate that treat the actin gel as an elastic continuum [23,40] and do not consider individual filaments. In such models, network growth creates elastic stress in the tail and deforms the gel, thereby squeezing the bacterium. As the stress in the gel is relaxed, the bacterium is pushed forward. This leads to a nonlinearity such that the bacterium can be pushed forward at a rate much faster than the polymerization rate. The force-velocity relations are obtained by assuming a force balance between the external drag, the elastic forces generated due to gel growth and an internal opposing force, which behaves like friction at low velocities in that it is proportional to the velocity. This opposing force arises from the binding and unbinding of filaments with finite bond elasticity. The model produces a shallow force velocity curve, such that the amount of force required to slow down the load appreciably is around one nanonewton. Based on the elastic modulus of the actin gel, this is the force scale required to significantly deform the gel. Forces of tens of piconewtons will not be sufficient to slow the moving load, similar to the observations by Wiesner *et al.* [15] and contrary to those by McGrath *et al.* [37]. As the internal opposing force increases, the force-velocity curve becomes shallower, the bacterium slows down, the filament density increases and the gel becomes thicker, which increases the stress buildup and consequently the driving force. The gel thickness is found to be in agreement with electron microscopy observations [31].

Further Implications for Models

While the models discussed above account for basic observations from biomimetic experiments, such as the force-velocity relations and their dependence on various parameters, the link between microscopic and macroscopic models needs to be explored. Two specific experimental findings, the binding of the actin tail to the surface of the load and the symmetry breaking resulting in directional movement, can be used to make refinements to the models. Recent experiments with lipid vesicles deformed by actin polymerization highlight the importance of the elastic interactions between the actin tail and the load [17,18].

Models for Binding

Experimental evidence of filament attachment constrains theoretical models that try to explain polymerization based motility and force generation. The recent experiments of Wiesner *et al.* [15] imply the existence of an internal force that might arise due to the attachment of filaments to the load surface. One important parameter that needs to be determined is the number of attached filaments that is sufficient to generate the observed retarding force. Electron microscopy reveals only a few filaments being attached to the bead [52]. This is consistent with only a few 'working' filaments being required to generate a force and to cause motility, as was implemented in the 'tethered Brownian ratchet' model [20]. However, the exact nature of the binding and the time scale of bond formation and dissociation in this system are unknown. The elastic model by Gerbal *et al.* [23] was one of the first to explicitly consider the binding between the tail and the bacterium. This model introduces the concept of an effective force that arises from the binding between the growing gel and the bacterial surface and opposes the polymerization force. As the stress increases and reaches a critical value, catastrophic breakage of bonds occurs, resulting in the bacterium hopping forward. A physical analogy is the slipping of a wet bar of soap when it is squeezed between two hands. An alternative model of 'clamped filament elongation' [58] also requires binding between actin and the membrane. Recent experiments with lipid vesicles indicate that the binding to the load surface should be an important feature in such models. In both experiments, moving vesicles deform to a characteristic teardrop shape, which is maintained as the vesicle moves, implying that some filaments are strongly bound [17,18]. This binding is sufficient to overcome the restoring force due to membrane stretching, which is typically in the range of a few nanonewtons for the vesicles used. The stepping motility of some vesicles is an extreme demonstration of the strength of binding and may be used to quantify it, if the density of filaments is known [17]. Careful experiments at the single filament level are required to directly measure these binding strengths.

Flexible Load

None of the models proposed so far has considered the effects of a flexible load like a membrane, which is most relevant at the leading edge of migrating cells. The elastic properties of the membrane, as well as its deformations, will affect the dynamics of polymerization. Experimental evidence from the study of actin propelled lipid vesicles suggests that the retractile forces are acting at the trailing edge and the protrusive forces are located on the sides ([17,18], Box 1). This implies that a majority of 'attached' or tethered filaments would be at the trailing edge and most of the free or 'working' filaments would be at the sides. The fluidity of the membrane may also play a role in this spatial segregation. Therefore, Brownian ratchet like models that consider polymerization of single filaments should be modified to include a flexible membrane. In order to describe the possible curvature dependent distribution of filament populations,

further experiments that look more closely at the interface between the actin and the membrane might provide important insight into the spatial organization of filaments near the membrane. A deterministic model [17] simulates the polymerization of actin, the consequent movement of the membrane and calculates the stress distribution on the deformed vesicle based on its stretching and volume change. However, the stochastic nature of the polymerization, elastic properties of the actin gel, nature of the viscous forces between the actin and membrane, and the different types of filament, bound and unbound to the membrane, remain to be considered.

Mechanism of Symmetry Breaking

A complete and self-consistent model must be able to explain the mechanism behind the spontaneous symmetry breaking that is observed in bead motility. A stochastic model [12] treating the actin filaments as elastic Brownian ratchets [19] suggests that the spontaneous symmetry breaking is caused by cooperative polymerization of neighboring filaments. The bead effectively couples the polymerization of different filament tips, such that filaments on the same side of the bead cooperate with each other, whereas filaments on opposite sides of the bead inhibit each other's growth. This arrangement allows for small stochastic fluctuations to be amplified leading to symmetry-breaking in the system [12]. A stochastic version of the tethered Brownian ratchet model [20] also displays the symmetry-breaking behavior. However, its dependence on parameters such as bead size was not calculated. The macroscopic elastic gel model [39] predicts that, above a critical value, growth induced stress in the gel will lead to a fracture in the gel, which can induce unidirectional motion by the development of a comet tail. The symmetry breaking threshold and the probability of fracture depend on the material properties of the gel as well as on the density of nucleators on the bead and the cross-linking density in the tail. Extending this idea, the time required to break symmetry was estimated as a function of the bead diameter and compared with experimental data [14]. It appears that significant stress can build up to induce symmetry breaking and to decrease the polymerization velocity. Experiments with phospholipid vesicles show a much faster symmetry breaking and possibly employ a different mechanism. More detailed experiments that follow the development of the actin tail around the vesicle surface would be able to clarify the mechanisms that underlie symmetry breaking, such as lateral diffusion of actin-associated proteins on the membrane surface. Such experiments may play a vital role in constructing models to follow the development of spatial polarity in cells.

Future Directions

The reductionist approach using biomimetic systems has fostered fruitful interactions between biochemists, cell biologists and physicists to streamline our understanding of the biophysical mechanisms and the key biochemical steps governing force generation by actin polymerization. Biomimetic systems, although important in their own right, are but a step towards our understanding of the more complicated problem of eukaryotic cell motility. The next challenge is to translate our understanding into events at the lamellipodium. While several features of biomimetic systems appear to play a role in a cellular environment, there are striking differences. Compared to biomimetic systems, the geometry of a cell is inverted, with the actin inside. Clearly, the geometry of biomimetic systems must be inverted into an artificial lamellipodium whose physical properties are under experimental control. Observations indicate that cells may regulate dynamical processes, for example, spreading and extension, by modulating the physical properties of the plasma membrane such as curvature or tension [59]. Alteration of membrane composition in specific regions of the cell surface may be controlled by signal transduction cascades, enabling the cell to initiate motility and maintain polarization. Biomimetic vesicles have the potential to probe how membrane properties couple to molecular networks that control motility or shape changes. As these reduced systems facilitate modeling to validate assumptions using quantitative experiments and mathematical analysis, they hopefully will provide exciting avenues of research that will help us to pin down the biophysical basis of cell motion.

Acknowledgements

We would like to thank George Oster, Jeffery Chabot and Hyman Carrel for critically reviewing the manuscript. This work was supported by National Science CAREER Grant PHY-0094181 and a MIT Pappalardo Fellowship in Physics.

References

1. Bray, D. (2001). Cell movements (Garland Publishing, New York).
2. Mitchison, T.J. and Cramer, L.P. (1996). Actin-based cell motility and cell locomotion. Cell *84*, 371–379.
3. Lauffenburger, D.A. and Horwitz, A.F. (1996). Cell migration: a physically integrated molecular process. Cell *84*, 359–369.
4. Pollard, T.D. and Borisy, G.G. (2003). Cellular motility driven by assembly and disassembly of actin filaments. Cell *112*, 453–465.
5. Pantaloni, D., Le Clainche, C. and Carlier, M.F. (2001). Mechanism of actin-based motility. Science *292*, 1502–1506.
6. Tilney, L.G. and Portnoy, D.A. (1989). Actin filaments and the growth, movement and spread of the intracellular bacterial parasite, Listeria monocytogenes. J. Cell Biol. *109*, 1597–1608.
7. Dramsi, S. and Cossart, P. (1998). Intracellular pathogens and the actin cytoskeleton. Annu. Rev. Cell Dev. Biol. *14*, 137–166.
8. Cameron, L.A., Giardini, P.A., Soo, F.S. and Theriot, J.A. (2000). Secrets of actin-based motility revealed by a bacterial pathogen. Nat. Rev. Mol. Cell Biol. *1*, 110–119.
9. Kocks, C., Marchand, J.B., Gouin, E., d'Hauteville, H., Sansonetti, P.J., Carlier, M.F. and Cossart, P. (1995). The unrelated surface proteins ActA of Listeria monocytogenes and IcsA of Shigella flexneri are sufficient to confer actin-based motility on Listeria innocua and Escherichia coli respectively. Mol. Microbiol. *18*, 413–423.
10. Loisel, T.P., Boujemaa, R., Pantaloni, D. and Carlier, M.F. (1999). Reconstitution of actin-based motility of Listeria and Shigella using pure proteins. Nature *401*, 613–616.
11. Cameron, L.A., Footer, M.J., van Oudenaarden, A. and Theriot, J.A. (1999). Motility of ActA protein-coated microspheres driven by actin polymerization. Proc. Natl. Acad. Sci. U.S.A. *96*, 4908–4913.
12. van Oudenaarden, A. and Theriot, J.A. (1999). Cooperative symmetry-breaking by actin polymerization in a model for cell motility. Nat. Cell Biol. *1*, 493–499.
13. Yarar, D., To, W., Abo, A. and Welch, M.D. (1999). The Wiskott-Aldrich syndrome protein directs actin-based motility by stimulating actin nucleation with the Arp2/3 complex. Curr. Biol. *9*, 555–558.

14. Bernheim-Groswasser, A., Wiesner, S., Golsteyn, R.M., Carlier, M.F. and Sykes, C. (2002). The dynamics of actin-based motility depend on surface parameters. Nature *417*, 308–311.

15. Wiesner, S., Helfer, E., Didry, D., Ducouret, G., Lafuma, F., Carlier, M.F. and Pantaloni, D. (2003). A biomimetic motility assay provides insight into the mechanism of actin-based motility. J. Cell Biol. *160*, 387–398.

16. Carlier, M.F., Clainche, C.L., Wiesner, S. and Pantaloni, D. (2003). Actin-based motility: from molecules to movement. Bioessays *25*, 336–345.

17. Upadhyaya, A., Chabot, J.R. andreeva, A., Samadani, A. and Van Oudenaarden, A. (2003). Probing polymerization forces by using actin-propelled lipid vesicles. Proc. Natl. Acad. Sci. U.S.A. *100*, 4521–4526.

18. Giardini, P.A., Fletcher, D.A. and Theriot, J.A. (2003). Compression forces generated by actin comet tails on lipid vesicles. Proc. Natl. Acad. Sci. U.S.A. *100*, 6493–6498.

19. Mogilner, A. and Oster, G. (1996). Cell motility driven by actin polymerization. Biophys. J. *71*, 3030–3045.

20. Mogilner, A. and Oster, G. (2003). Force generation by actin polymerization II: the elastic ratchet and tethered filaments. Biophys. J. *84*, 1591–1605.

21. Carlsson, A.E. (2001). Growth of branched actin networks against obstacles. Biophys. J. *81*, 1907–1923.

22. Carlsson, A.E. (2003). Growth velocities of branched actin networks. Biophys. J. *84*, 2907–2918.

23. Gerbal, F., Chaikin, P., Rabin, Y. and Prost, J. (2000). An elastic analysis of Listeria monocytogenes propulsion. Biophys. J. *79*, 2259–2275.

24. Machesky, L.M. and Insall, R.H. (1998). Scar1 and the related Wiskott-Aldrich syndrome protein, WASP, regulate the actin cytoskeleton through the Arp2/3 complex. Curr. Biol. *8*, 1347–1356.

25. Rohatgi, R., Ma, L., Miki, H., Lopez, M., Kirchhausen, T., Takenawa, T. and Kirschner, M.W. (1999). The interaction between N-WASP and the Arp2/3 complex links Cdc42-dependent signals to actin assembly. Cell *97*, 221–231.

26. Higgs, H.N. and Pollard, T.D. (2001). Regulation of actin filament network formation through ARP2/3 complex: activation by a diverse array of proteins. Annu. Rev. Biochem. *70*, 649–676.

27. Gittes, F., Mickey, B., Nettleton, J. and Howard, J. (1993). Flexural rigidity of microtubules and actin filaments measured from thermal fluctuations in shape. J. Cell Biol. *120*, 923–934.

28. Ott, A., Magnasco, M., Simon, A. and Libchaber, A. (1993). Measurement of the persistence length of polymerized actin using fluorescence microscopy. Physical Review. E. Statistical Physics, Plasmas, Fluids and Related Interdisciplinary Topics *48*, R1642–R1645.

29. Isambert, H., Venier, P., Maggs, A.C., Fattoum, A., Kassab, R., Pantaloni, D. and Carlier, M.F. (1995). Flexibility of actin filaments derived from thermal fluctuations. Effect of bound nucleotide, phalloidin and muscle regulatory proteins. J. Biol. Chem. *270*, 11437–11444.

30. Borisy, G.G. and Svitkina, T.M. (2000). Actin machinery: pushing the envelope. Curr. Opin. Cell Biol. *12*, 104–112.

31. Tilney, L.G., DeRosier, D.J. and Tilney, M.S. (1992). How Listeria exploits host cell actin to form its own cytoskeleton. I. Formation of a tail and how that tail might be involved in movement. J. Cell Biol. *118*, 71–81.

32. Blanchoin, L., Amann, K.J., Higgs, H.N., Marchand, J.B., Kaiser, D.A. and Pollard, T.D. (2000). Direct observation of dendritic actin filament networks nucleated by Arp2/3 complex and WASP/Scar proteins. Nature *404*, 1007–1011.

33. Pantaloni, D., Boujemaa, R., Didry, D., Gounon, P. and Carlier, M.F. (2000). The Arp2/3 complex branches filament barbed ends: functional antagonism with capping proteins. Nat. Cell Biol. *2*, 385–391.

34. Amann, K.J. and Pollard, T.D. (2001). The Arp2/3 complex nucleates actin filament branches from the sides of pre-existing filaments. Nat. Cell Biol. *3*, 306–310.

35. Hill, T.L. and Kirschner, M.W. (1982). Bioenergetics and kinetics of microtubule and actin filament assembly-disassembly. Int. Rev. Cytol. *78*, 1–125.

36. Dogterom, M. and Yurke, B. (1997). Measurement of the force-velocity relation for growing microtubules. Science *278*, 856–860.

37. McGrath, J.L., Eungdamrong, N.J., Fisher, C.I., Peng, F., Mahadevan, L., Mitchison, T.J. and Kuo, S.C. (2003). The force-velocity relationship for the actin-based motility of Listeria monocytogenes. Curr. Biol. *13*, 329–332.

38. Gerbal, F., Laurent, V., Ott, A., Carlier, M.F., Chaikin, P. and Prost, J. (2000). Measurement of the elasticity of the actin tail of Listeria monocytogenes. Eur. Biophys. J. *29*, 134–140.

39. Noireaux, V., Golsteyn, R.M., Friederich, E., Prost, J., Antony, C., Louvard, D. and Sykes, C. (2000). Growing an actin gel on spherical surfaces. Biophys. J. *78*, 1643–1654.

40. Sackmann, E. (1995). In Structure and Dynamics of Membranes, R. Lipowsky and E. Sackmann, eds. (Amsterdam: Elsevier), pp. 213-304.

41. Evans, E. and Rawicz, W. (1990). Entropy-driven tension and bending elasticity in condensed-fluid membranes. Phys. Rev. Lett. *64*, 2094–2097.

42. Miyata, H. and Hotani, H. (1992). Morphological changes in liposomes caused by polymerization of encapsulated actin and spontaneous formation of actin bundles. Proc. Natl. Acad. Sci. U.S.A. *89*, 11547–11551.

43. Miyata, H., Nishiyama, S., Akashi, K. and Kinosita, K., Jr. (1999). Protrusive growth from giant liposomes driven by actin polymerization. Proc. Natl. Acad. Sci. U.S.A. *96*, 2048–2053.

44. Cortese, J.D., Schwab, B., 3rd, Frieden, C. and Elson, E.L. (1989). Actin polymerization induces a shape change in actin-containing vesicles. Proc. Natl. Acad. Sci. U.S.A. *86*, 5773–5777.

45. Merrifield, C.J., Moss, S.E., Ballestrem, C., Imhof, B.A., Giese, G., Wunderlich, I. and Almers, W. (1999). Endocytic vesicles move at the tips of actin tails in cultured mast cells. Nat. Cell Biol. *1*, 72–74.

46. Ma, L., Cantley, L.C., Janmey, P.A. and Kirschner, M.W. (1998). Corequirement of specific phosphoinositides and small GTP-binding protein Cdc42 in inducing actin assembly in Xenopus egg extracts. J. Cell Biol. *140*, 1125–1136.

47. Taunton, J., Rowning, B.A., Coughlin, M.L., Wu, M., Moon, R.T., Mitchison, T.J. and Larabell, C.A. (2000). Actin-dependent propulsion of endosomes and lysosomes by recruitment of N-WASP. J. Cell Biol. *148*, 519–530.

48. Italiano, J.E., Jr., Roberts, T.M., Stewart, M. and Fontana, C.A. (1996). Reconstitution *in vitro* of the motile apparatus from the amoeboid sperm of Ascaris shows that filament assembly and bundling move membranes. Cell *84*, 105–114.

49. Abraham, V.C., Krishnamurthi, V., Taylor, D.L. and Lanni, F. (1999). The actin-based nanomachine at the leading edge of migrating cells. Biophys. J. *77*, 1721–1732.

50. Kuo, S.C. and McGrath, J.L. (2000). Steps and fluctuations of Listeria monocytogenes during actin-based motility. Nature *407*, 1026–1029.

51. Lasa, I., Gouin, E., Goethals, M., Vancompernolle, K., David, V., Vandekerckhove, J. and Cossart, P. (1997). Identification of two regions in the N-terminal domain of ActA involved in the actin comet tail formation by Listeria monocytogenes. EMBO J. *16*, 1531–1540.

52. Cameron, L.A., Svitkina, T.M., Vignjevic, D., Theriot, J.A. and Borisy, G.G. (2001). Dendritic organization of actin comet tails. Curr. Biol. *11*, 130–135.

53. Nabi, I.R. (1999). The polarization of the motile cell. J. Cell Sci. *112*, 1803–1811.

54. Pistor, S., Chakraborty, T., Walter, U. and Wehland, J. (1995). The bacterial actin nucleator protein ActA of Listeria monocytogenes contains multiple binding sites for host microfilament proteins. Curr. Biol. *5*, 517–525.

55. Chakraborty, T., Ebel, F., Domann, E., Niebuhr, K., Gerstel, B., Pistor, S., Temm-Grove, C.J., Jockusch, B.M., Reinhard, M., Walter, U., et al. (1995). A focal adhesion factor directly linking intracellularly motile Listeria monocytogenes and Listeria ivanovii to the actin-based cytoskeleton of mammalian cells. EMBO J. *14*, 1314–1321.

56. Reinhard, M., Halbrugge, M., Scheer, U., Wiegand, C., Jockusch, B.M. and Walter, U. (1992). The 46/50 kDa phosphoprotein VASP purified from human platelets is a novel protein associated with actin filaments and focal contacts. EMBO J. *11*, 2063–2070.

57. Peskin, C.S., Odell, G.M. and Oster, G.F. (1993). Cellular motions and thermal fluctuations: the Brownian ratchet. Biophys. J. *65*, 316–324.

58. Dickinson, R.B. and Purich, D.L. (2002). Clamped-filament elongation model for actin-based motors. Biophys. J. *82*, 605–617.

59. Raucher, D. and Sheetz, M.P. (2000). Cell spreading and lamellipodial extension rate is regulated by membrane tension. J. Cell Biol. *148*, 127–136.